# Recent developments of radial integration boundary element method in solving nonlinear and nonhomogeneous multi-size problems

X. W. Gao [1], M. Cui [1] and Ch. Zhang [2]

[1] School of Aeronautics and Astronautics, State Key Laboratory of Structural Analysis for Industrial Equipment, Dalian University of Technology, PR China,

E-mails: xwgao@dlut.edu.cn; miaocui@dlut.edu.cn

[2] Department of Civil Engineering, University of Siegen, D-57068 Siegen, Germany,

E-mail: c.zhang@uni-siegen.de

**Keywords:** Boundary element method; Radial integration method; Nearly singular integrals, Thin structures

**Abstract** This paper presents some recent developments of the meshless boundary element method based on radial integration method (RIM) for solving 2D and 3D heat transfer and thermoelasticity problems. Special attention is paid to the consideration of the effects such as structural multi-sizes, nonlinear, non-homogeneous, and anisotropic problems. Firstly, general boundary-domain integral equations for heat conduction and stress analysis are derived using the weighted residual method based on the source point isolation technique, in which fundamental solutions for the corresponding linear homogeneous problems are adopted. The use of linear isotropic fundamental solutions for anisotropic, nonlinear and nonhomogeneous problems results in domain integrals appearing in the basic integral equations. The domain integrals appearing in the integral equations, then, are transformed into equivalent boundary integrals using RIM, resulting in a pure boundary element analysis algorithm without the need of internal cells. The thermal and mechanical material properties can be the functions of both temperature (resulting in nonlinear heat transfer) and spatial coordinates (for non-homogeneous materials). The Newton-Raphson iteration scheme is applied to solve the resulting nonlinear equation set. The nearly singular boundary integrals stemming from treating thin-structures using BEM are evaluated using the non-equally spaced element sub-division technique. The three-step solver of multi-domain BEM is employed to solve composite structural problems consisting of different materials. Finally, numerical examples are given to demonstrate the accuracy and efficiency of the presented method.

## 1. Introduction

Thin structures are frequently used in aerospace engineering [1], such as multi-layered coatings, laminated structures, honeycomb structures etc. The investigation shows that the thermal stresses induced in laminated structures are the main cause of structural failure [2]. Therefore, the thermal stress analysis of composite structures is significantly important in aerospace engineering. The boundary element method (BEM) has distinctive advantages in solving problems of fracture mechanics [3] and thin structural problems [4], since it only needs to discretize the boundary of the problem into elements. However, the conventional BEM is not so attractive in solving nonhomogeneous, nonlinear and thermoelasticity problems, since domain integrals are inevitably introduced in the resulting integral equations [5]. A direct evaluation of domain integrals requires the discretization of the domain into internal cells. This severely eliminates the advantage of BEM. To overcome this disadvantage, Nardini and Brebbia [6] developed the dual reciprocity method (DRM) to transform the domain integrals into equivalent boundary integrals. To avoid using particular solutions required in the DRM, Gao proposed the radial integration method (RIM) [7] which can transform any domain integrals to the boundary based on a pure mathematical manipulation. RIM has been successfully applied to solve thermoelasticity [8], elastic inclusion [9], and creep damage mechanics problems [10]. In view of the robustness and simplicity of RIM in evaluating domain integrals without using internal cells, Hematiyan [11] gave a very good assessment to RIM, and Albuquerque et al. [12] compared RIM to DRM numerically through applications to dynamic problems with a more positive conclusion.

Although thermoelasticity problems with constant material properties have been solved using the boundary-only element method based on RIM [8], this methodology has yet not been applied to solve heat conduction

and thermoelastic thin structure problems with varying material properties. This paper is an attempt for this purpose. First, boundary-domain integral equations for temperature and displacements are derived from the weighted residual forms of governing equations. Then, the domain integrals arising in the integral equations are transformed into equivalent boundary integrals using RIM, resulting in a pure boundary element solution algorithm. Material properties are allowed to be any type of functions of spatial coordinates. The treatment of nearly singular integrals is a challenge issue in solving thin structural problems using BEM [13]. A non-equally spaced element sub-division technique is presented for evaluating the nearly singular integrals. Numerical examples are given to demonstrate the correctness and efficiency of the presented method.

## 2. Boundary-domain integral equations for general nonlinear and nonhomogenous heat conduction problems

### 2.1. Formulations for general heat conduction problems

The governing equation for general heat conduction problems can be expressed as

$$\frac{\partial}{\partial x_i}\left(k_{\mathrm{ij}}\frac{\partial T}{\partial x_j}\right)+Q=0\,, \tag{1}$$

where $k_{\mathrm{ij}}$ and $Q$ are the thermal property tensor and the source term, respectively, and $T$ denotes the temperature. $k_{\mathrm{ij}}$ and $T$ both may be functions of spatial coordinates for non-homogeneous problems or functions of the temperature for non-linear problems. It is noted that the thermal property tensor is symmetric, i.e., $k_{\mathrm{ij}}=k_{\mathrm{ji}}$. The repeated subscripts in eq (1) represent summation over the ranges of their values. Using a weight function $G$ to multiply both sides of eq (1) and integrating over the entire domain $\Omega$, the following weak-form can be written.

$$\int_{\Omega} G\frac{\partial}{\partial x_i}\left(k_{\mathrm{ij}}\frac{\partial T}{\partial x_j}\right)d\Omega+\int_{\Omega} GQd\Omega=0\,. \tag{2}$$

The first integral can be manipulated as follows

$$\begin{aligned}\int_{\Omega} G\frac{\partial}{\partial x_i}\left(k_{\mathrm{ij}}\frac{\partial T}{\partial x_j}\right)d\Omega &= \int_{\Gamma} Gk_{\mathrm{ij}}\frac{\partial T}{\partial x_j}n_{\mathrm{i}}d\Gamma-\int_{\Omega}\frac{\partial G}{\partial x_i}k_{\mathrm{ij}}\frac{\partial T}{\partial x_j}d\Omega\\ &=-\int_{\Gamma} Gqd\Gamma-\int_{\Gamma} q^{*}Td\Gamma+\bar{\int}_{\Omega}\frac{\partial}{\partial x_j}\left(k_{\mathrm{ij}}\frac{\partial G}{\partial x_i}\right)Td\Omega\\ &=-\int_{\Gamma} Gqd\Gamma-\int_{\Gamma} q^{*}Td\Gamma+I_{\Omega}\,,\end{aligned} \tag{3}$$

where

$$q=-k_{\mathrm{ij}}\frac{\partial T}{\partial x_j}n_{\mathrm{i}}\,,\qquad q^{*}=\frac{\partial G}{\partial x_i}k_{\mathrm{ij}}n_{\mathrm{j}}\,, \tag{4}$$

$$I_{\Omega}=\bar{\int}_{\Omega}\frac{\partial}{\partial x_j}\left(k_{\mathrm{ij}}\frac{\partial G}{\partial x_i}\right)Td\Omega\,, \tag{5}$$

in which $\Gamma$ denotes the boundary of the domain $\Omega$, $n_i$ is the $i$-th component of the outward normal vector to $\Gamma$, and $q$ is the heat flux. It is noted that the domain integral in eq (5) may be strongly singular (depending on the choice of $G$) and, therefore, a different integral symbol is used to denote this.

We assume that the weight function $G$ is a fundamental solution of either isotropic or anisotropic problems. Usually, it is a function of the distance $r$ between the source point $p$ and the field point $q$ [14]. When $r\to 0$, $G$ may be singular and, therefore, an infinitesimal circular domain $\Omega_{\varepsilon}$ centered at the source point $p$ with radius $\varepsilon$ can be isolated from $\Omega$ (Fig. 1).

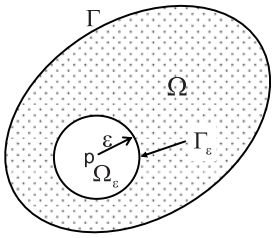


Fig. 1 An infinitesimal domain $\Omega_\varepsilon$ isolated from $\Omega$

The last term in eq (3) now can be written as

$$\begin{aligned} I_\Omega &= \int_\Omega \frac{\partial}{\partial x_j}\left(k_{ij}\frac{\partial G}{\partial x_i}\right)T d\Omega = \lim_{\varepsilon\to 0}\int_{\Omega_\varepsilon}\frac{\partial}{\partial x_j}\left(k_{ij}\frac{\partial G}{\partial x_i}\right)T d\Omega + \lim_{\varepsilon\to 0}\int_{\Omega-\Omega_\varepsilon}\frac{\partial}{\partial x_j}\left(k_{ij}\frac{\partial G}{\partial x_i}\right)T d\Omega \\ &= T(p)\lim_{\varepsilon\to 0}\int_{\Omega_\varepsilon}\frac{\partial}{\partial x_j}\left(k_{ij}\frac{\partial G}{\partial x_i}\right)d\Omega + \int_\Omega \frac{\partial}{\partial x_j}\left(k_{ij}\frac{\partial G}{\partial x_i}\right)T d\Omega = -k(p)T(p) + \int_\Omega V T d\Omega, \end{aligned} \tag{6}$$

where

$$k(p) = -\lim_{\varepsilon\to 0}\int_{\Omega_\varepsilon}\frac{\partial}{\partial x_i}\left(k_{ij}\frac{\partial G}{\partial x_j}\right)d\Omega = -\lim_{\varepsilon\to 0}\int_{\Gamma_\varepsilon} k_{ij}\frac{\partial G}{\partial x_j}n_i d\Gamma = -k_{ij}(p)\lim_{\varepsilon\to 0}\int_{\Gamma_\varepsilon}\frac{\partial G}{\partial x_i}n_j d\Gamma,, \tag{7}$$

$$V = \frac{\partial}{\partial x_i}\left(k_{ij}\frac{\partial G}{\partial x_j}\right) = \frac{\partial k_{ij}}{\partial x_i}\frac{\partial G}{\partial x_j} + k_{ij}\frac{\partial^2 G}{\partial x_i \partial x_j}. \tag{8}$$

It is noted that the last domain integral in eq (6) is interpreted in the Cauchy principal value sense. Substituting eq (6) into eq (3) and the result into eq (2) yields

$$kT + \int_\Gamma q^* T d\Gamma = -\int_\Gamma G q d\Gamma + \int_\Omega V T d\Omega + \int_\Omega G Q d\Omega. \tag{9}$$

Equation (9) is a boundary-domain integral equation valid for isotropic, anisotropic, linear and nonlinear heat conduction problems. The weight function $G$ can be any type of functions. If $G$ is a regular function, the coefficient $k$ as determined by eq (7) will be zero since the radius $\varepsilon \to 0$; if $G$ is chosen as the Green's function [14] which is weakly singular when the source point $p$ approaches the field point $q$ under integration, $k$ has a finite value; and if $G$ is chosen as a higher singular function than the Green's function, $k$ is infinite and, therefore, this type of $G$ doesn't make sense. Once the weight function $G$ and thermal property tensor $k_{ij}$ are given, all coefficients and kernel functions in eq (9) are known, and the unknown quantities be computed using the standard BEM discretization procedure [5].

It is noted that although eq (9) is derived for an internal source point $p$, it can also be used for boundary nodes since it is actually not necessary to compute the coefficient $k$ directly using eq (7). This is based on the fact that the contribution of $k$ to the final system of equations is in the diagonal term, which can be determined using a more efficient way, i.e., the "rigid body motion condition" [5].

### 2.2 Using isotropic fundamental solutions for general anisotropic heat conduction problems

In principle, the weight function $G$ can be any function. However, the simplest way is to choose $G$ as the Green's function for isotropic heat conduction problems, i.e.,

$$G = \begin{cases} \dfrac{1}{2\pi}\ln\left(\dfrac{1}{r}\right), & 2D, \\ \dfrac{1}{4\pi r}, & 3D, \end{cases} \tag{10}$$

where $r$ is the distance between the source point $p$ and field point $q$. The derivatives of $G$ can be expressed as

$$\frac{\partial G}{\partial x_i} = \frac{-1}{2\pi\alpha r^{\alpha}} r_{,i}, \tag{11}$$

$$\frac{\partial^2 G}{\partial x_i \partial x_j} = \frac{-1}{2\pi\alpha r^{\beta}} (\delta_{ij} - \beta r_{,i} r_{,j}), \tag{12}$$

where $r_{,i} = \partial r / \partial x_i$, $\beta=2$ for 2D and $\beta=3$ for 3D problems, and $\alpha=\beta-1$. Since $\Gamma_\varepsilon$ is a circle (2D) or a sphere (3D), we have $n_{,j} = r_{,j}$. Thus, from eq (7) it follows that

$$k = \frac{k_{ij}}{2\pi\alpha} \int_{\Gamma_\varepsilon} \frac{r_{,i} n_j}{r^{\alpha}} d\Gamma = \frac{k_{ij}}{2\pi\alpha} \int_{\Gamma_\varepsilon} \frac{r_{,i} r_{,j}}{r^{\alpha}} d\Gamma . \tag{13}$$

For an internal point, using the following relationship [5]

$$\int_{\Gamma_\varepsilon} \frac{r_{,i} r_{,j}}{r^{\alpha}} d\Gamma = \begin{cases} \pi\delta_{ij}, & 2D, \\ \dfrac{4\pi}{3}\delta_{ij}, & 3D, \end{cases} \tag{14}$$

equation (13) can be integrated as

$$k = k_{ii} / \beta . \tag{15}$$

It can be seen that $k$ is the average value of the diagonal term of $k_{ij}$. This is helpful for understanding the coefficient $k$ in eq (9). It is also pointed out that if the problem is isotropic, the last term in eq (8) is zero and eq (9) is reduced to the result in [14].

## 3. Boundary-domain integral equations for thermoelasticity with variable coefficients

The governing equations of the thermoelasticity problems can be expressed as [8]

$$\sigma_{ij} = \mu C^0_{ijkl} u_{k,l} - \delta_{ij} \tilde{\alpha} T , \tag{16}$$

where

$$\tilde{\alpha} = \frac{2(1+\nu)\mu\bar{\alpha}}{1-2\nu}, \tag{17}$$

$$C^0_{ijkl} = \frac{2\nu}{1-2\nu}\delta_{ij}\delta_{kl} + \delta_{ik}\delta_{jl} + \delta_{il}\delta_{jk}, \tag{18}$$

in which $\mu$ represents the shear modulus, $\nu$ the Poisson's ratio, $\bar{\alpha}$ the thermal expansion coefficient, and $u_k$ the displacement components. Both $\mu$ and $\bar{\alpha}$ are functions of temperature and spatial coordinates.

Through applying the weighted residual method [8,15] to eq (16), the following boundary-domain integral equations for the displacements and the stresses can be obtained

$$\begin{aligned} \tilde{u}_i(\boldsymbol{y}) = & \int_\Gamma U_{ij}(\boldsymbol{x},\boldsymbol{y}) t_j(\boldsymbol{x}) d\Gamma(\boldsymbol{x}) - \int_\Gamma T_{ij}(\boldsymbol{x},\boldsymbol{y}) \tilde{u}_j(\boldsymbol{x}) d\Gamma(\boldsymbol{x}) \\ & + \int_\Omega V_{ij}(\boldsymbol{x},\boldsymbol{y}) \tilde{u}_j(\boldsymbol{x}) d\Omega(\boldsymbol{x}) + \int_\Omega U_{ij,j}(\boldsymbol{x},\boldsymbol{y}) \hat{T}(\boldsymbol{x}) d\Omega(\boldsymbol{x}), \end{aligned} \tag{19}$$

$$\begin{aligned} \sigma_{ij}(\boldsymbol{y}) = & \int_\Gamma U_{ijk}(\boldsymbol{x},\boldsymbol{y}) t_k(\boldsymbol{x}) d\Gamma(\boldsymbol{x}) - \int_\Gamma T_{ijk}(\boldsymbol{x},\boldsymbol{y}) \tilde{u}_k(\boldsymbol{x}) d\Gamma(\boldsymbol{x}) \\ & + \int_\Omega V_{ijk}(\boldsymbol{x},\boldsymbol{y}) \tilde{u}_k(\boldsymbol{x}) d\Omega(\boldsymbol{x}) + \int_\Omega \Psi_{ij}(\boldsymbol{x},\boldsymbol{y}) [\hat{T}(\boldsymbol{x}) - \hat{T}(\boldsymbol{y})] \, d\Omega(\boldsymbol{x}) \\ & + \hat{T}(\boldsymbol{y}) \int_\Gamma r \ln r \frac{\partial r}{\partial n} \Psi_{ij}(\boldsymbol{x},\boldsymbol{y}) d\Gamma(\boldsymbol{x}) - \delta_{ij} h \hat{T}(\boldsymbol{y}) + F_{ijk}(\boldsymbol{y}) \tilde{u}_k(\boldsymbol{y}), \end{aligned} \tag{20}$$

where $U_{ij}$, $T_{ij}$, $V_{ij}$, $U_{ijk}$, $T_{ijk}$, $V_{ijk}$ and $F_{ijk}$ can be found in [15], and other quantities are given by

$$\widetilde{u}_j = \mu u_j, \tag{21}$$

$$\hat{T} = \frac{2(1+\nu)\mu\overline{\alpha}}{1-2\nu} T, \tag{22}$$

$$\Psi_{ij} = \frac{(1-2\nu)}{2\alpha\pi(1-\nu)r^{\beta}}(\delta_{ij} - \beta r_{,i} r_{,j}), \tag{23}$$

$$h = \frac{(1+\beta)(1-2\nu)}{6(1-\nu)}. \tag{24}$$

Equations (19) and (20) are only suitable for internal points. For boundary nodes, a limiting process is needed to establish the boundary integral equations from eq (19), and the "Traction-Recovery Method" [5] is adopted to compute the boundary stresses.

## 4. Evaluation of nearly singular integrals using a non-equally spaced element sub-division technique

When solving thin-structure problems using BEM, the treatment of nearly singular integrals is a challenge issue [4-6,13]. The element sub-division technique is a simple and robust technique in handling such problems [16] with the advantage of treating various orders of singularities using a unified way. Gao and Davies [5] proposed an equally-spaced element sub-division technique for evaluating the nearly singular integrals. The technique is simple, however, when the source point is very close to the element under integration, the number of sub-elements is huge and the computational time is intolerable. In this study, a non-equally spaced element sub-division technique is presented, which is able to reduce the computational time by several magnitude of orders for the same accuracy. The technique is based on a relationship proposed by Gao and Davies [16] for Gaussian quadrature regarding the number of Gaussian points, the minimum distance to element and the element size.

The Gaussian quadrature formula for surface integrals can be expressed as [17]:

$$I = \sum_{i=1}^{m_1}\sum_{j=1}^{m_2} w_i^1 w_j^2 f(\xi_1^i, \xi_2^j) + E_1 + E_2, \tag{25}$$

where $(\xi_1^i, \xi_2^j)$ are the Gaussian point coordinates, $w_i^1$ and $w_j^2$ are the weighting factors, $m_1$ and $m_2$ are the numbers of Gaussian points, and $E_1$ and $E_2$ are the integration errors, i.e.,

$$E_i = \frac{L_i^{2m_i+1}(m_i!)^4}{(2m_i+1)[(2m_i)!]^3} f^{2m_i}, \tag{26}$$

in which $f^{2m_i}$ denotes the $2m_i$-th derivative of the function $f$, $L_i$ is the length of the element in the $i$-th direction. From eq (25) it can be seen that the integration error relies on the number of Gaussian points and the element length. Therefore, to ensure a desired accuracy, a big element must be divided into small sub-elements. Based on the analysis of an upper bound of the relative error, Mustoe [17] presented the following approximate formula for the specified accuracy tolerance $e$

$$2\left(\frac{L_i}{4R}\right)^{2m_i} \frac{(2m_i+p-1)!}{(2m_i)!(p-1)!} \le e, \tag{27}$$

where $p$ is the singularity order of the integral kernel characterized by $r^{-p}$, $R$ is the minimum distance from the source point to the element. Equation (27) shows that, to retain the specified accuracy $e$ and the number of Gaussian points cannot exceed a given number, the value of $L_i/R$ needs to be reduced by dividing the big element into a number of sub-elements. Based on the numerical investigation, Gao and Davies [16, 5] proposed the following formula for determining the number of Gaussian points.

$$m_i = \frac{p' \log_e (e/2)}{2 \log_e \left[ L_i / (4R) \right]}, \tag{28}$$

where

$$p' = \sqrt{\frac{2}{3} p + \frac{2}{5}}. \tag{29}$$

After a rearrangement eq (28) yields

$$L_i = 4R \left( \frac{e}{2} \right)^{\frac{p'}{2m_i}}. \tag{30}$$

Equation (28) can be used to determine the minimum number of Gaussian points for a given accuracy tolerance $e$, while eq (30) can be used to determine the length of each sub-element for the specified values of allowed maximum number of Gaussian points, singularity order and the minimum distance. The non-equally spaced element sub-division technique can be summarized as follows:

1) Compute length $L_i$ of the boundary element under integration and the minimum distance $R$ from the source point **y** to the element. Detailed Fortran subroutines for determining $L_i$ and $R$ can be found in [5].
2) Calculate the required number of Gaussian points $m_i$ using eq (28) in terms of the values of $L_i$ and $R$.
3) If $m_i \le m_{\max}$ ($m_{\max}$ being the specified maximum number of Gaussian points), evaluate integrals using Gaussian quadrature formulas.
4) If $m_i > m_{\max}$, let $m_i = m_{\max}$ and compute the length $L_i^n$ of each sub-element along the integration direction $i$ using the value of $R$ and eq (30).
5) As shown in Fig. 2, mark the graduations in two integration directions in terms of $L_1^n$ and $L_2^n$ and form all sub-elements (enclosed by dashed lines) from these graduations.
6) Evaluate integrals over each sub-element using Gaussian quadrature formulas.

For understanding this process easily, Fig. 2 gives the schematic show of a big boundary element divided into 12 sub-elements by partitioning the line along $\xi_1$ direction into 4 segments and the line along $\xi_2$ direction into 3 segments.

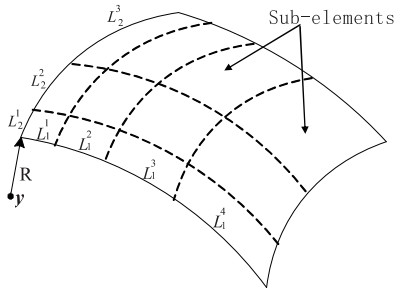


Fig. 2 Schematic show of the element sub-division

## 5. Numerical examples

Based on the method described in the paper, a computer code named BERIM (Boundary Element analysis based on Radial Integration Method) has been developed. In the code, all domain integrals appearing in eqs (9), (19) and (20) have been transformed into boundary integrals using RIM [7], resulting in a pure boundary element analysis algorithm without need of internal cells. When the material properties are functions of the temperature, the Newton-Raphson iteration scheme is applied to solve the nonlinear heat conduction equations. To solve composite structure problems, the three-step multi-domain BEM (MDBEM) solver proposed in [18] is adopted for both heat conduction and thermoelasticity problems. Corner and edge points are treated using the discontinuous elements to model the discontinuity of the heat flux and the traction. Two

numerical examples are presented in the following.

**5.1 Thermal stress analysis over a honeycomb structure**

The first example is a honeycomb structure which is commonly used in thermal protection system (TPS) [1]. The structure consists of upper and lower cover plates with a thickness of 0.125mm. The honeycomb core has a wall thickness of 0.035mm, a wall height of 7.11mm, and a width of 4.76mm. The structure has a total of 100 honeycombs with the global dimension of 49.98mm × 42.56mm × 7.36mm. Figure 3 shows the BEM model consisting of 8946 four-noded boundary and interface elements with 8484 nodes. In the BEM model, the upper and lower plates, the honeycomb wall, and the hollow volume filling with air are treated as different sub-domains. The heat conductivities are $7.8\times10^{-5}$ W/(mm·K) for the upper and lower plates, $1.7\times10^{-4}$ W/(mm·K) for the honeycomb wall, and $2.3\times10^{-5}$ W/(mm·K) for the filled air. The thermal boundary conditions are given as follows:

the top and bottom surfaces are specified with the temperature distribution of $T(x,y,z)=-\dfrac{225xz}{49.98\times7.36}-\dfrac{75x}{49.98}+\dfrac{600z}{7.36}+200$ (K) and the side surfaces are adiabatic.

Firstly, the heat conduction computation is performed to obtain the temperature distribution in the structure, and then the thermoelasticity computation is carried out using the obtained temperature. In the thermoelasticity computation, the material parameters are taken as $\mu$=280GPa, $\nu$=0.25, and the thermal expansion coefficient is $\overline{\alpha}=2.47\times10^{-6}$mm/K . The top surface is uniformly imposed by traction conditions of $\tau_x$=0.05MPa and $\tau_z$=-0.5MPa, the bottom surface is fixed, and the side surface is traction-free. Figure 5 shows the computed temperatures at points shown in Fig. 4, which are located below the inner surface of the upper plate with a distance of 0.01mm to the inner surface. The computed heat flux $q_z$, displacement $u_x$ and stress $\sigma_{xx}$ at these selected points are presented in Figs. 6, 7 and 8, respectively.

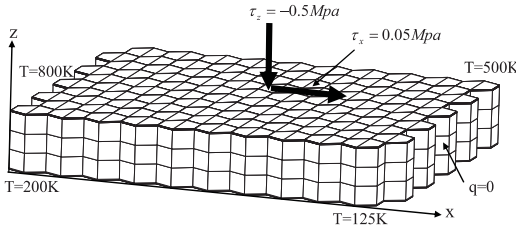


Fig. 3 BEM model and boundary conditions

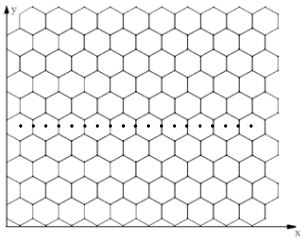


Fig. 4 Points for results plotting

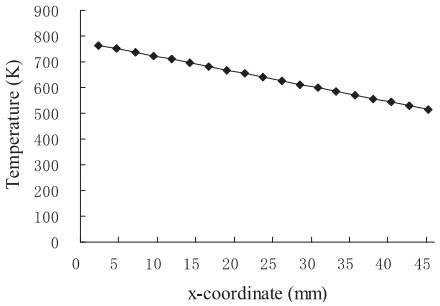


Fig. 5 Distribution of temperature

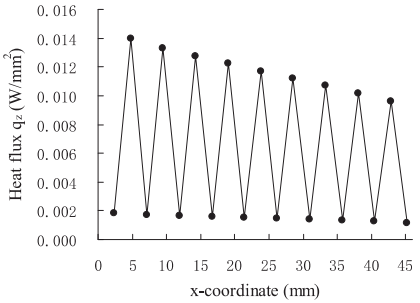


Fig. 6 Distribution of heat flux $q_z$

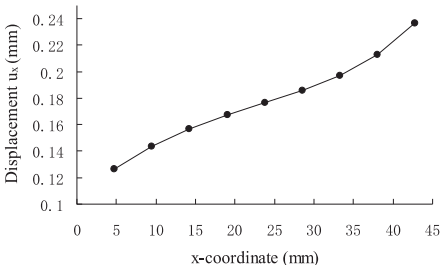


Fig. 7 Displacement $u_x$

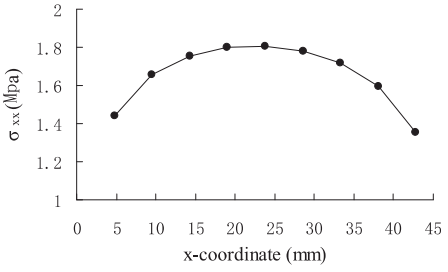


Fig. 8 Stress $\sigma_{xx}$

From Fig. 6, we can see that the heat flux $q_z$ has a much larger value on the honeycomb side wall than in the hollow air. This important phenomenon captured in the example is attributed to the discretization of the two surfaces of the honeycomb wall into boundary elements. Figure 8 shows that the computed stress $\sigma_{xx}$ is much larger than the imposed tractions. This indicates that the thermal stress is an important factor in TPS failure analysis.

**5.2 Rectangular plate with a crack under tensile loading**

The second example analyzed is a rectangular plate with an edge crack, which is subjected to a uniform tensile loading as depicted in Fig. 9. The geometry of the cracked plate is described by: plate width $b$=10, plate length $2h$=30 and crack-length $a$=0.4$b$. To demonstrate the capability of the presented method to treat the crack problem, a single computational domain is used in our computation. The upper and lower surfaces of the crack is very close, but not completely in contact, measured with the width ratio of the opening distance to the crack-length $a$. The boundary of the plate including the crack surfaces is discretized into 115 quadratic boundary elements with 254 boundary nodes. Two nodes are defined at the crack-tip for utilizing the discontinuous element [18] to model the discontinuity of the traction across the tip. Plain strain condition is assumed in our computation.

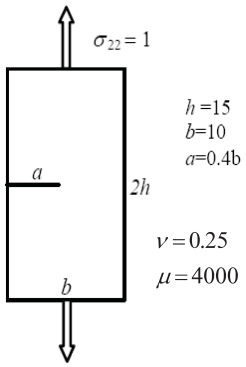


Fig. 9 A plate with an edge crack

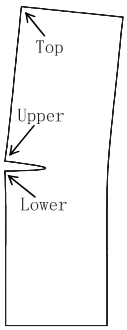


Fig. 10 Deformed plate

Figure 10 shows the deformed plate plotted using the computed displacements multiplied by a factor of 200 for the case of the width ratio being 0.1%. To verify the correctness, this problem is also computed using the multi-domain BEM code [18], in which lower and upper parts of the plate are treated as two sub-domains along the crack. The displacements in $y$-direction computed using the present single domain method denoted by "1-Domain" and using the multi-domain BEM denoted by "2-Domain" are listed in Table 1 for three corner nodes as shown in Fig. 10. Comparison of the results from the two methods shows that the relative errors are rather small. To investigate the convergence of the computational results to the width of the crack, computations are carried out using different ratios of the crack-width to the crack-length. The computed results for the three selected corner nodes (see Fig. 10) are shown in Fig. 11. From Fig. 11, it can be seen

that the convergence is achieved when the width ratio is larger than 0.02% which is small enough to model a real crack-width. Figure 11 also shows that the usual single domain BEM combined with the non-equally spaced element sub-division technique described in this paper can solve the crack problems efficiently without the use of other complicated methods [3, 18].

Table 1 Computed displacement $u_y$ at three selected nodes

| | Lower | Upper | Top |
|---|---|---|---|
| 1-Domain | 8.66874E-4 | 5.7889E-3 | 6.6526E-3 |
| 2-Domain | 8.75949E-4 | 5.7325E-3 | 6.6045E-3 |
| Error (%) | -1.04 | 0.984 | 0.728 |

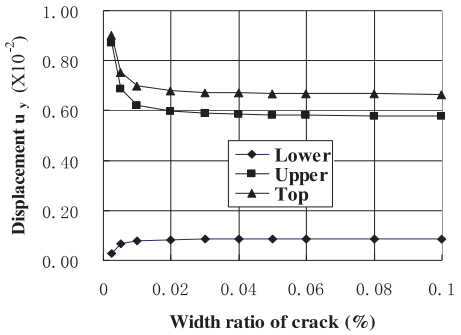


Fig. 11 Displacement computed using different values of the crack-width

## 6. Conclusions

A boundary element technique is presented for solving 2D and 3D nonlinear and non-homogeneous heat transfer and thermoelasticity problems. A non-equally spaced element sub-division technique is proposed for evaluating nearly singular boundary integrals in the analysis of thin structures using BEM. Numerical results show that the presented method can not only effectively solve the thin-wall structure problems, but can also solve crack problems in the usual way. This is very convenient to solve complicated engineering problems.

## References

[1] Myers D.E., Martin C,J., Blosser M.L., Parametric weight comparison of advanced metallic, ceramic tile, and ceramic blanket thermal protection systems. NASA/TM-2000-210289, 2000.

[2] Hohe J., Goswami S., Becker W., Assessment of interface stress concentrations in layered composites with application to sandwich panels. *Computational Materials Science*, 2002, **26**: 71-79.

[3] Chen J.T., Hong H.K., Review of dual boundary element methods with emphasis on hypersingular integrals and divergent series. *Applied Mechanics Reviews, ASME*, 1999, **52**(1): 17-33.

[4] Luo J.F., Liu Y.J., Berger E.J., Analysis of two-dimensional thin structures (from micro- to nano-scales) using the boundary element method. Computational Mechanics, 1998, **22**: 404-412.

[5] Gao X.W., Davies T.G., *Boundary Element Programming in Mechanics*. Cambridge, London, New York: Cambridge University Press, 2002.

[6] Nardini D., Brebbia C.A., A new approach for free vibration analysis using boundary elements. In: Brebbia C.A., editor. *Boundary Element Methods in Engineering*. Berlin: Springer, 1982, 312-326.

[7] Gao X.W., The radial integration method for evaluation of domain integrals with boundary-only discretization. *Engineering Analysis with Boundary Elements*, 2002, **26**: 905-916.

[8] Gao X.W., Boundary element analysis in thermoelasticity with and without internal cells. *International Journal for Numerical Methods in Engineering*, 2003, **57**: 975-990.

[9] Dong C.Y., Lo S.H., Cheung Y.K., Numerical solution for elastic inclusion problems by domain integral equation with integration by means of radial basis functions. *Engineering Analysis with Boundary Elements*, 2004, **28**: 623-632.

[10] Gun H., 3D boundary element analysis of creep continuum damage mechanics problems. *Engineering Analysis with Boundary Elements*, 2005, **29**: 749-755.
[11] Hematiyan M.R., A general method for evaluation of 2D and 3D domain integrals without domain discretization and its application in BEM. *Computational Mechanics*, 2007, **39**: 509-520.
[12] Albuquerque E.L., Sollero P., Paiva W.P., The radial integration method applied to dynamic problems of anisotropic plates. *Commun. Numer. Meth. Eng.*, 2007, **23**: 805-818.
[13] Niu Z., Cheng C., Zhou H., Hu Z., Analytic formulations for calculating nearly singular integrals in two-dimensional BEM. Engineering Analysis with Boundary Elements, 2007, **31**: 949-964.
[14] Gao X.W., A meshless BEM for isotropic heat conduction problems with heat generation and spatially varying conductivity. *Int. J. Numer. Meth. Engng.,* 2008, **66**: 1411-1431.
[15] Gao X.W., Zhang Ch., Guo L., Boundary-only element solutions of 2D and 3D nonlinear and nonhomogeneous elastic Problems. *Engineering Analysis with Boundary Elements*, 2007, **31**: 974-982.
[16] Gao X.W., Davies T.G., Adaptive algorithm in elasto-plastic boundary element analysis. *Journal of the Chinese Institute of Engineers* (English edition), 2000, **23**(3): 349-356.
[17] Mustoe G.G.W., Advanced integration schemes over boundary elements and volume cells for two- and three-dimensional non-linear analysis. In: *Development in Boundary Element Methods*, Elsevier, London, 1984.
[18] Gao X.W., Guo L., Zhang Ch., Three-step multi-domain BEM solver for nonhomogeneous material problems. *Engineering Analysis with Boundary Elements*, 2007, **31**: 965-973.